

Flavor asymmetry of polarized antiquark distributions and semi-inclusive DIS

B. Dressler^{1,a}, K. Goeke^{1,b}, M.V. Polyakov^{1,2,c}, C. Weiss^{1,d}

¹ Institut für Theoretische Physik II, Ruhr-Universität Bochum, 44780 Bochum, Germany

² Petersburg Nuclear Physics Institute, Gatchina, St.Petersburg 188350, Russia

Received: 30 November 1999 / Published online: 17 March 2000 – © Springer-Verlag 2000

Abstract. The $1/N_c$ -expansion of QCD suggests large flavor asymmetries of the polarized antiquark distributions in the nucleon. This is confirmed by model calculations in the large- N_c limit (chiral quark-soliton model), which give sizable results for $\Delta\bar{u}(x) - \Delta\bar{d}(x)$ and $\Delta\bar{u}(x) + \Delta\bar{d}(x) - 2\Delta\bar{s}(x)$. We compute the contributions of these flavor asymmetries to the spin asymmetries in hadron production in semi-inclusive deep-inelastic scattering. We show that the large flavor asymmetries predicted by the chiral quark-soliton model are consistent with the recent HERMES data for spin asymmetries in charged hadron production.

1 Introduction

The study of polarized parton distributions in the nucleon presents a major challenge to both experiment and theory. Particularly subtle issues are the polarized antiquark distributions, and the precise flavor decomposition of the polarized quark and antiquark distributions, including the strangeness contributions. Knowledge of the latter is a prerequisite e.g. for the identification of the gluon contribution to the proton spin [1].

Traditional inclusive lepton scattering experiments, i.e., measurements of the polarized structure functions, do not allow to directly distinguish between the polarized quark- and antiquark distributions. Rather, quark- and antiquark contributions have to be identified from the study of scaling violations, which implies a considerable loss of accuracy [2]. Moreover, the flavor decomposition can only be studied by way of comparing experiments with different targets, typically proton and light nuclei (deuteron, helium), which is rendered difficult by nuclear binding effects. Much more direct access to the individual quark- and antiquark distributions is possible in polarized semi-inclusive DIS (deep-inelastic scattering), where one measures e.g. the spin asymmetry of the cross section for producing a certain hadron in the fragmentation of the struck quark or antiquark in the target [3]. Such measurements have recently been performed by the SMC [4] and HERMES [5] experiments. The unpolarized quark and antiquark fragmentation functions needed in the QCD description of these asymmetries can be measured independently in e^+e^- -annihilation into hadrons [6], and also

in hadron production in unpolarized DIS off the nucleon [7, 8].

There have also been attempts to estimate the flavor asymmetry of the polarized antiquark distributions theoretically, using models for the structure of the nucleon. A large flavor asymmetry of the polarized antiquark distribution was first obtained in a calculation of the quark- and antiquark distributions at a low scale in the large- N_c limit (N_c is the number of colors), where the nucleon can be described as a soliton of an effective chiral theory [9–11]. The unpolarized quark- and antiquark distributions [9, 10, 12], as well as the polarized distributions of quarks plus antiquarks [9, 10, 13] calculated in this approach are in good agreement with the standard parametrizations obtained from fits to inclusive DIS data [2]. In the $1/N_c$ -expansion the isovector polarized distributions are leading compared to the isoscalar ones, and calculations in the chiral quark-soliton model, using standard parameters, give an isovector antiquark distribution, $\Delta\bar{u}(x) - \Delta\bar{d}(x)$, considerably larger than the isoscalar one, $\Delta\bar{u}(x) + \Delta\bar{d}(x)$. Such a large polarized antiquark flavor asymmetry should lead to observable effects in semi-inclusive spin asymmetries as measured e.g. by the HERMES experiment. It should be noted that the same approach describes well the observed violation of the Gottfried sum rule [14–16] and the recent data for the x -dependence of the flavor asymmetry of the unpolarized antiquark distribution from Drell-Yan pair production [17] and semi-inclusive DIS [18], see [12, 11, 19] for details.

Recently, the polarized antiquark flavor asymmetry has been estimated in approaches which generalize the meson cloud picture of DIS off the nucleon to the polarized case [20, 21]. It is known that pion exchange contributions to DIS off the nucleon provide a qualitative explanation for the observed flavor asymmetry of the unpolarized antiquark distribution [22, 23]. In [20] the authors considered

^a e-mail: birgيتد@tp2.ruhr-uni-bochum.de

^b e-mail: goeke@tp2.ruhr-uni-bochum.de

^c e-mail: maximp@tp2.ruhr-uni-bochum.de

^d e-mail: weiss@tp2.ruhr-uni-bochum.de

the contribution of polarized rho meson exchange to the polarized antiquark distributions in the nucleon and obtained an estimate of the flavor asymmetry considerably smaller than the large- N_c result of [9,10].

In this paper we offer new arguments in favor of a large flavor asymmetry of the polarized antiquark distributions. Our main points are two: First, on the theoretical side, we comment on the estimates of the polarized flavor asymmetry in the meson exchange picture in [20,21]. Specifically, we argue that the polarized rho meson exchange contributions considered in [20] are not the dominant contributions within that approach, so that a small value obtained for this contribution does not imply smallness of the total polarized antiquark flavor asymmetry. Second, we study the implications of the flavor asymmetry of the polarized antiquark distributions for the spin asymmetries measured in hadron production in semi-inclusive DIS. Combining information on the polarized quark and antiquark distributions available from inclusive DIS with the large- N_c model calculation of the polarized flavor asymmetries, we make quantitative predictions for the spin asymmetries in semi-inclusive pion, kaon, and charged particle production. We discuss the sensitivity of these observables to the flavor asymmetries of the polarized antiquark distributions. With the quantitative estimate of $\Delta\bar{u}(x) - \Delta\bar{d}(x)$ from the chiral quark soliton model we obtain a sizable contribution of the flavor asymmetry to semi-inclusive spin asymmetries. Actually, incorporating the effects of the large flavor asymmetry our results fit well the recent HERMES data for spin asymmetries in semi-inclusive charged hadron production [5]. We discuss the assumptions made in the analysis of the HERMES data in [5], and argue that they are too restrictive and might have led to a bias in favor of a small flavor asymmetry. We also make predictions for experiments with the possibility to measure spin asymmetries of individual charged hadrons (π^+ , π^- , K^+ , K^-), which could be feasible at HERMES or CEBAF.

2 Flavor asymmetry of the polarized antiquark distribution in the large- N_c limit

Quark- and antiquark distributions in the large- N_c limit. A very useful tool for connecting QCD with the hadronic world is the theoretical limit of a large number of colors. Qualitatively speaking, at large N_c QCD becomes equivalent to a theory of mesons, with baryons appearing as solitonic excitations [24]. The $1/N_c$ -expansion allows to classify baryon and meson masses, weak and strong characteristics in a model-independent way; usually the estimates agree surprisingly well with phenomenology. One example are the isovector and isoscalar axial coupling constants of the nucleon, which are of the order

$$g_A^{(3)} \sim N_c, \quad g_A^{(0)} \sim N_c^0, \quad (1)$$

in qualitative agreement with the numerical values extracted from experiments, $g_A^{(3)} \approx 1.25$ and $g_A^{(0)} \approx 0.3$.

The same technique has been applied to the parton distributions in the nucleon at a low normalization point [9]. There one finds that the isoscalar unpolarized and the isovector polarized distributions of quarks and antiquarks are leading in the $1/N_c$ -expansion, while the respective other flavor combinations, the isovector unpolarized and isoscalar polarized distributions, appear only in the next-to-leading order. More precisely, at large N_c the distributions scale as

leading:

$$\left. \begin{array}{l} u(x) + d(x), \quad \bar{u}(x) + \bar{d}(x) \\ \Delta u(x) - \Delta d(x), \quad \Delta\bar{u}(x) - \Delta\bar{d}(x) \end{array} \right\} \sim N_c^2 f(N_c x), \quad (2)$$

subleading:

$$\left. \begin{array}{l} u(x) - d(x), \quad \bar{u}(x) - \bar{d}(x) \\ \Delta u(x) + \Delta d(x), \quad \Delta\bar{u}(x) + \Delta\bar{d}(x) \end{array} \right\} \sim N_c f(N_c x), \quad (3)$$

where $f(y)$ is a stable function in the large N_c -limit, which depends on the particular distribution considered. Note that the large N_c -behavior of the polarized quark- and antiquark distributions is related to that of the corresponding axial coupling constants, (1) by the sum rules for the first moments of these distributions (Bjorken and Ellis-Jaffe sum rules).

It is interesting that the isovector polarized antiquark distribution is parametrically larger than the isoscalar one. While the $1/N_c$ -expansion is only a parametric estimate, it is nevertheless an indication that $\Delta\bar{u}(x) - \Delta\bar{d}(x)$ could be also numerically large. This is indeed confirmed by model calculations (see below).

Polarized vs. unpolarized antiquark flavor asymmetry. We would like to briefly comment on the assumptions about the polarized antiquark flavor asymmetry made in the recent analysis of the HERMES data for semi-inclusive DIS [5]. From the point of view of the $1/N_c$ -expansion the flavor asymmetry of the polarized antiquark distribution is parametrically larger than that of the unpolarized ones. Thus, the assumption in the fit of [5] of proportional flavor asymmetry in the polarized and unpolarized antiquark distributions, namely $\Delta\bar{u}(x)/\bar{u}(x) = \Delta\bar{d}(x)/\bar{d}(x)$, is inconsistent with the $1/N_c$ -expansion and appears unnatural. The consequences of this assumption can be seen more clearly if one notes that it implies

$$\Delta\bar{u}(x) - \Delta\bar{d}(x) = [\bar{u}(x) - \bar{d}(x)] \frac{\Delta\bar{u}(x) + \Delta\bar{d}(x)}{\bar{u}(x) + \bar{d}(x)}. \quad (4)$$

The ratio of the isoscalar polarized to the isoscalar unpolarized distribution on the R.H.S. is always less than unity, which follows from the probabilistic interpretation of the leading-order distributions considered here. Thus, with the above assumption the polarized antiquark flavor asymmetry can never be larger numerically than the unpolarized one. Consequently, a fit under the assumption $\Delta\bar{u}(x)/\bar{u}(x) = \Delta\bar{d}(x)/\bar{d}(x)$ cannot be regarded as a

real alternative to the reference fit assuming zero polarized antiquark flavor asymmetry, $\Delta\bar{u}(x) - \Delta\bar{d}(x) = 0$. In this sense it seems that the analysis of [5] contained an implicit bias in favor of a small polarized antiquark flavor asymmetry.

Model calculation of quark and antiquark distributions at a low normalization point. In order to make quantitative estimates of the parton distributions at a low normalization point one needs to supplement the large- N_c limit with some dynamical information. It is known that at low energies the behavior of strong interactions is largely determined by the spontaneous breaking of chiral symmetry. A concise way to summarize the implications of this non-perturbative phenomenon is by way of an effective field theory, valid at low energies. Such a theory has been derived “microscopically” within the framework of the instanton description of the QCD vacuum, which provides a dynamical explanation for the breaking of chiral symmetry in QCD [25]. It can be expressed in terms of an effective Lagrangian describing quarks with a dynamical mass, interacting with pions, which appear as Goldstone bosons in the spontaneous breaking of chiral symmetry (here x denotes the space-time coordinates):

$$L_{\text{eff}} = \bar{\psi}(x) [i\gamma^\mu \partial_\mu - M U^{\gamma_5}(x)] \psi(x), \quad (5)$$

$$U^{\gamma_5}(x) \equiv \frac{1 + \gamma_5}{2} U(x) + \frac{1 - \gamma_5}{2} U^\dagger(x). \quad (6)$$

Here $U(x)$ is a unitary matrix containing the Goldstone boson degrees of freedom, which can be parametrized as

$$U(x) = \frac{1}{F_\pi} [\sigma(x) + i\tau^a \pi^a(x)], \quad \sigma^2 + (\pi^a)^2 = F_\pi^2. \quad (7)$$

($F_\pi = 93 \text{ MeV}$ is the weak pion decay constant). The effective theory is valid up to an ultraviolet cutoff, whose value is of the order 600 MeV [25].

In the large- N_c limit the nucleon in the effective theory defined by (5) is described by a classical pion field which binds the quarks (chiral quark-soliton model) [26]. The field is of “hedgehog” form; in the nucleon rest frame it is given by

$$U_{\text{cl}}(\mathbf{x}) = \exp \left[i \frac{x^a \tau^a}{r} P(r) \right], \quad r \equiv |\mathbf{x}|, \quad (8)$$

where $P(r)$ is called the profile function; $P(0) = -\pi$, and $P(r) \rightarrow 0$ for $r \rightarrow \infty$. Nucleon states with definite spin/isospin and momentum emerge after quantizing the collective rotations and translations of the soliton. The parton distributions in the nucleon at large N_c can be computed by summing over the contributions of quark single-particle states in the background field; the normalization point is of the order of the ultraviolet cutoff of the effective theory, $\mu \approx 600 \text{ MeV}$ (see [9, 10] for details).

Gradient expansion of the isovector polarized antiquark distribution. Analytic expressions for the parton distributions in the large- N_c nucleon can be obtained in the theoretical limit of large soliton size, where one can perform an expansion of the sum over quark levels in gradients of

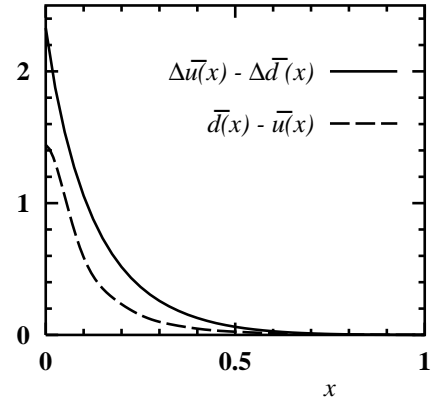


Fig. 1. *Solid line:* The isovector polarized antiquark distribution at the low normalization point ($\mu = 600 \text{ MeV}$), as obtained from the chiral soliton model of the nucleon (for details see the text). *Dashed line:* The isovector unpolarized antiquark distribution calculated in [12]

the classical pion field, (8) [9]. The isovector polarized antiquark distribution in leading-order gradient expansion is given by

$$\begin{aligned} \Delta\bar{u}(x) - \Delta\bar{d}(x) &= \frac{F_\pi^2 M_N}{3} \int_{-\infty}^{\infty} \frac{d\xi \cos M_N \xi x}{2\pi \xi} \\ &\times \int d^3y \text{tr} \left[\tau^3 (-i) U_{\text{cl}}(\mathbf{y} + \xi \mathbf{e}_3) U_{\text{cl}}^\dagger(\mathbf{y}) \right] \\ &= \frac{4M_N}{3} \int_{-\infty}^{\infty} \frac{d\xi \cos M_N \xi x}{2\pi \xi} \\ &\times \int d^3y \pi_{\text{cl}}^3(\mathbf{y} + \xi \mathbf{e}_3) \sigma_{\text{cl}}(\mathbf{y}), \end{aligned} \quad (9)$$

where M_N denotes the nucleon mass, \mathbf{e}_3 the three-dimensional unit vector in the 3-direction, and τ^3 the isospin Pauli matrix.¹ The reason why we are interested in this theoretical limit is that it allows to make explicit the dependence of the polarized antiquark distribution on the classical chiral fields of the soliton. This will be useful for the discussion in Sect. 3. Aside from this, comparison with the result of exact numerical calculations shows that the leading-order gradient expansion, (9), gives already a very realistic numerical estimate of the isovector polarized antiquark distribution [10].

Numerical result for $\Delta\bar{u}(x) - \Delta\bar{d}(x)$. In the numerical estimates of semi-inclusive asymmetries in Sect. 4 we shall use not the gradient expansion formula, (9), but a more accurate numerical estimate obtained by adding the bound-state level contribution and using interpolation-type formula to estimate the continuum contribution [9]. This result for the distribution is shown in Fig. 1. One sees

¹ We remark that, when combined with the corresponding gradient expansion expression for the isovector polarized quark distribution, the first moment of (9) reproduces the well-known expression for the gradient expansion of the isovector axial coupling constant, $g_A^{(3)}$, of the large- N_c nucleon.

that the flavor asymmetry of the polarized antiquark distribution is numerically larger than the unpolarized one [12], in agreement with the fact that it is leading in the $1/N_c$ -expansion. Note that the unpolarized antiquark flavor asymmetry calculated in this approach is in agreement with the results of the analysis of the E866 Drell–Yan data [17] as well as with the HERMES measurements in semi-inclusive DIS [18] (for details, see [12,11,19]).

Including strangeness. For a realistic description of semi-inclusive spin asymmetries one has to take into account the polarized distribution of strange quarks and antiquarks in the nucleon. Within the large- N_c description of the nucleon it is possible to include strangeness by extending the effective low-energy theory in the chiral limit, (5) to three quark flavors and treating corrections due to the finite strange current quark mass perturbatively. In this approach the nucleon is described by embedding the $SU(2)$ hedgehog, (8), in the $SU(3)$ flavor space, and quantizing its flavor rotations in the full $SU(3)$ flavor space. Flavor symmetry breaking can then be included perturbatively by computing matrix elements of symmetry-breaking operators between $SU(3)$ -symmetric nucleon states [27]. For our estimates here we limit ourselves to the simplest case of unbroken $SU(3)$ symmetry ($m_s = 0$). In this case collective quantization of the $SU(3)$ rotations of the soliton leads to a simple relation between the flavor-octet and triplet polarized antiquark distributions, namely

$$\begin{aligned} \Delta\bar{u}(x) + \Delta\bar{d}(x) - 2\Delta\bar{s}(x) \\ = \frac{3F - D}{F + D} [\Delta\bar{u}(x) - \Delta\bar{d}(x)]. \end{aligned} \quad (10)$$

The value of F/D has been estimated in the chiral quark soliton model [28]. When one regards the radius of the soliton as a free parameter (in reality it is determined from minimizing the energy of the soliton), the result for F/D interpolates between the $SU(6)$ quark model value (for small soliton size), $F/D = 2/3$, and the value obtained in the Skyrme model (for large soliton size), $F/D = 5/9$.² Using the value $F/D = 5/9$ corresponding to the limit of large soliton size, the ratio in (10) comes to $3/7$. We shall use the relation (10) with this value in our estimates of semi-inclusive spin asymmetries in Sect. 4.

3 On the flavor asymmetry of the polarized antiquark distribution in the meson cloud picture

A widely used phenomenological model for the flavor asymmetry of the unpolarized antiquark distributions in the nucleon is the meson cloud picture [23]. Recently there have been attempts to estimate also the polarized antiquark flavor asymmetry in this approach [20,21]. In particular, the authors of [20] obtained an estimate for $\Delta\bar{u}(x) -$

² It is interesting to note that in this approach the value for F/D is one-to-one related to the isoscalar axial coupling constant, $g_A^{(0)}$, see [28].

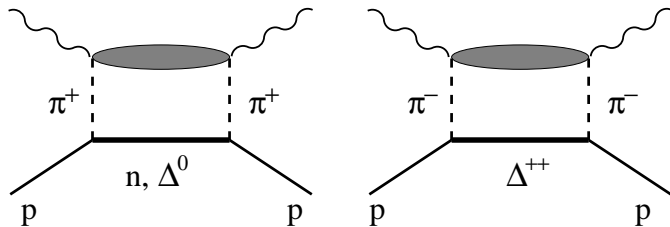


Fig. 2. The Sullivan mechanism contributing to the unpolarized antiquark flavor asymmetry in the proton, $\bar{u}(x) - \bar{d}(x)$

$\Delta\bar{d}(x)$ more than an order of magnitude smaller than the result of the large- N_c model calculation, Fig. 1. This striking disagreement may lead to the impression that the present theoretical understanding of the polarized antiquark flavor asymmetry is very poor. In this situation we consider it helpful to briefly comment on the estimates within the meson cloud picture. Specifically, we want to show how the very small estimate obtained in [20] could be reconciled with our large- N_c result. To avoid misunderstandings, we stress at this point that, in spite of many superficial similarities, the meson cloud picture described here differs in many crucial respects from the large- N_c approach (more on this below), so the two approaches should not be confused.

The meson cloud picture of DIS off the nucleon assumes that the nucleon can be described as a “bare” nucleon, characterized by flavor-symmetric quark- and antiquark distributions, and a “cloud” of virtual mesons. The flavor asymmetry of the antiquark distributions is then attributed to processes in which the hard probe couples to such a virtual meson. For instance, the sign of the observed unpolarized antiquark asymmetry in the proton, $\bar{d}(x) - \bar{u}(x) > 0$, can qualitatively be explained by the photon coupling to a pion in the “cloud” (Sullivan mechanism [22]), if one takes into account that the emission of a π^+ by the proton, with transition to a neutron or Δ^0 intermediate state, is favored compared to that of a π^- , which is possible only by a transition to a Δ^{++} state, as illustrated in Fig. 2.³

The simple Sullivan mechanism involving the pion “cloud” does not contribute to the polarized asymmetry, which has often been taken as an argument in favor of the smallness of this asymmetry. Recently, Boreskov and Kaidalov [21] made the interesting observation that at small x a sizable polarized antiquark asymmetry is generated by the interference of the amplitudes for the photon coupling to a pion and to a rho meson emitted by the nucleon, as shown schematically in Fig. 3. This type of exchange corresponds to the leading Regge cut contributing to the imaginary part of the high-energy photon-nucleon scattering amplitude. Previously, Fries and Schäfer [20] had considered the Sullivan-type contribution from polarized rho meson exchange to the polarized antiquark asymmetry, $\Delta\bar{u}(x) - \Delta\bar{d}(x)$, at larger values of x (i.e., not restricted to small x), see Fig. 4.

³ For a discussion of the role of the πNN and $\pi N\Delta$ form factors in quantitative estimates of these contributions, see [29].

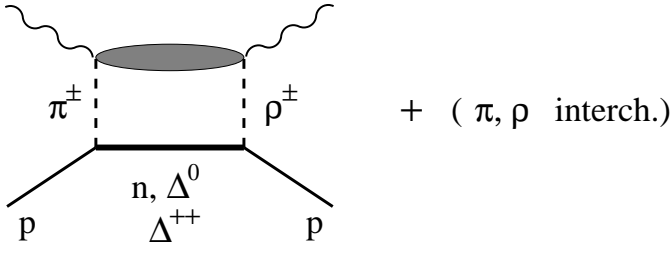


Fig. 3. The pi-rho interference contributions to the isovector polarized structure function at small x considered in [21]

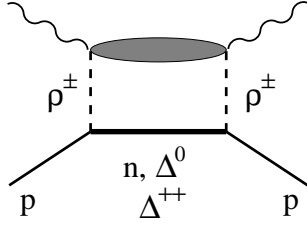


Fig. 4. The polarized rho meson exchange contributions to $\Delta\bar{u}(x) - \Delta\bar{d}(x)$ considered in [20]

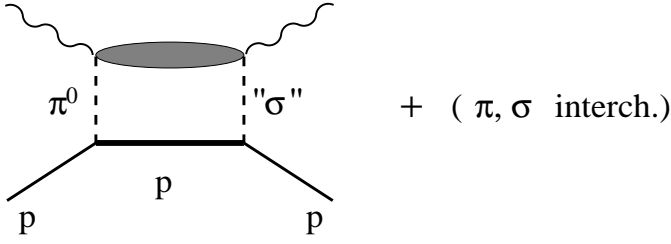


Fig. 5. Schematic illustration of the “pi-sigma” interference likely to give a large contribution to $\Delta\bar{u}(x) - \Delta\bar{d}(x)$ in the meson cloud picture (for details, see the text)

They obtained a strikingly small contribution to $\Delta\bar{u}(x) - \Delta\bar{d}(x)$, roughly two orders of magnitude smaller than the result of the calculation in the large- N_c limit shown in Fig. 1. It should be noted, however, that within the meson cloud picture contributions of type of Fig. 4 are not special. In fact, one can obtain a contribution to the polarized antiquark distribution already from the exchange of spin-0 mesons. To see this it is instructive to take a look at the gradient expansion of the isovector polarized antiquark distribution in large- N_c limit, (9). Although the fields in (9) are the classical chiral fields of the soliton, and no direct interpretation of this expression in terms of simple meson exchange diagrams is possible, it can provide some qualitative insights as to which quantum numbers can contribute to the polarized flavor asymmetry. Equation (9) suggests that, in the language of the meson cloud model, a contribution to the polarized antiquark asymmetry at average values of x should come already from the interference of pion and “sigma meson” exchange, as illustrated in Fig. 5.

Given the large mass of the rho meson compared to the pion, and the additional suppression due to need to have a polarized rho meson, it is not difficult to imagine that this interference contribution could give a much larger contri-

bution to $\Delta\bar{u}(x) - \Delta\bar{d}(x)$ than the Sullivan-type polarized rho meson exchange of Fig. 4.

It is difficult in QCD to meaningfully speak about exchanges of mesons other than pions, which play a special role as Goldstone bosons of spontaneously broken chiral symmetry, and as mediators of strong interactions at long distances.⁴ In a “pure” pion cloud picture, contributions of the type indicated in Fig. 5 should be referred to as interference between the photon scattering off a flavor-symmetric “bare” nucleon and a pion in the “cloud”.

We emphasize that the large- N_c results for the flavor asymmetries of the antiquark distributions in the nucleon cannot generally be interpreted as single meson exchange diagrams such as Figs. 2–5. This can be seen from the fact that the large- N_c limit of individual meson exchange diagrams typically gives rise to a wrong large- N_c behavior of the resulting quark and antiquark distributions, different from (2) and (3). The large- N_c approach avoids the arbitrary separation of nucleon structure functions into “core” and “cloud” contributions. At the same time, however, this approach retains the possibility of describing genuine Goldstone boson exchange contributions at large distances. For example, the large- N_c result for the helicity skewed quark distribution correctly reproduces the singularity found in this distribution in the chiral limit in QCD, which can be attributed to Goldstone boson exchange [30].

4 Semi-inclusive spin asymmetries

In leading-order QCD the spin asymmetry of the cross section for semi-inclusive production of a hadron of type h in the deep-inelastic scattering of a virtual photon off a hadronic target is given by

$$A_1^h(x, z; Q^2) = \frac{\sum_a e_a^2 \Delta q_a(x, Q^2) D_a^h(z, Q^2)}{\sum_b e_b^2 q_b(x, Q^2) D_b^h(z, Q^2)} \times \left[\frac{1 + R(x, Q^2)}{1 + \gamma^2} \right], \quad (11)$$

where x is the Bjorken variable, $Q^2 = -q^2$ the photon virtuality, and $q_a(x, Q^2)$ and $\Delta q_a(x, Q^2)$, denote, respectively, the unpolarized and polarized quark and antiquark distributions in the target, at the scale Q^2 . The sum over a, b implies the sum over light quark flavors as well as over quarks/antiquarks:

$$a, b = \{u, \bar{u}, d, \bar{d}, s, \bar{s}\}.$$

Furthermore, $D_a(z, Q^2)$ denotes the quark and antiquark fragmentation functions, describing the probability for the struck quark of type a to fragment into a hadron of type

⁴ It should be noted that even in the case of pure pion exchange, which can in principle be properly defined in the soft-pion limit, the notion of meson exchange contributions to the nucleon structure functions presents severe conceptual difficulties, since in graphs of the type of Fig. 2 the typical momenta of the exchanged pions are not small, but can run up to momenta of the order of ~ 1 GeV [29].

h with fraction z of its longitudinal momentum. Finally, in (11) $R(x, Q^2) = \sigma_L/\sigma_T$ is the usual ratio of the total longitudinal to the transverse photon cross section, and $\gamma = 2xM_N/\sqrt{Q^2}$ is a kinematical factor.

Instead of the spin asymmetry for fixed z , (11), one usually considers the so-called integrated asymmetry, which is defined as

$$A_1^h(x; Q^2) = \frac{\sum_a e_a^2 \Delta q_a(x; Q^2) D_a^h(Q^2)}{\sum_b e_b^2 q_b(x; Q^2) D_b^h(Q^2)} \times \left[\frac{1 + R(x, Q^2)}{1 + \gamma^2} \right], \quad (12)$$

where

$$D_a^h(Q^2) = \int_{z_{\min}}^1 dz D_a^h(z; Q^2). \quad (13)$$

Here $z_{\min} > 0$ is a cutoff which ensures that the observed hadron was in fact produced by fragmentation of the struck quark in the target (suppression of target fragmentation) [8].

Due to the presence of the (anti-) quark fragmentation functions in the expression for the asymmetries (11) and (12) the quark and antiquark distributions in the target enter with different coefficients. This is different from the inclusive spin asymmetry, which at the same level of approximation is given by

$$A_1(x, Q^2) = \frac{\sum_a e_a^2 \Delta q_a(x, Q^2)}{\sum_b e_b^2 q_b(x, Q^2)} \left[\frac{1 + R(x, Q^2)}{1 + \gamma^2} \right]. \quad (14)$$

[Up to kinematical factors this quantity is equal to the ratio of polarized to unpolarized structure functions, $g_1(x, Q^2)/F_1(x, Q^2)$]. In the following it will be convenient to rewrite the expression for the semi-inclusive asymmetry, (12), in such a way as to explicitly separate the contributions of those combinations of parton distributions which are known well from inclusive DIS, from others which discriminate between quark and antiquark distributions. We write

$$A_1^h(x; Q^2) = [A_{1,u}^h + A_{1,d}^h + A_{1,s}^h + A_{1,0}^h + A_{1,3}^h + A_{1,8}^h](x; Q^2), \quad (15)$$

where the contributions are defined as (we omit the Q^2 -dependence for brevity)

$$A_{1,u}^h(x) = X_u^h [\Delta u(x) + \Delta \bar{u}(x)] \quad (\text{analogously for } d, s), \quad (16)$$

$$A_{1,0}^h(x) = X_0^h [\Delta \bar{u}(x) + \Delta \bar{d}(x) + \Delta \bar{s}(x)], \quad (17)$$

$$A_{1,3}^h(x) = X_3^h [\Delta \bar{u}(x) - \Delta \bar{d}(x)], \quad (18)$$

$$A_{1,8}^h(x) = X_8^h [\Delta \bar{u}(x) + \Delta \bar{d}(x) - 2\Delta \bar{s}(x)]. \quad (19)$$

The coefficients X_u^h, \dots, X_8^h are given by the following combination of quark charges and quark fragmentation functions:

$$X_u^h(x) = \frac{e_u^2 D_u^h}{Y} \quad (\text{analogously for } d, s), \quad (20)$$

$$X_0^h = \frac{1}{3Y} [-e_u^2(D_u^h - D_{\bar{u}}^h) - e_d^2(D_d^h - D_{\bar{d}}^h) - e_s^2(D_s^h - D_{\bar{s}}^h)], \quad (21)$$

$$X_3^h = \frac{1}{2Y} [-e_u^2(D_u^h - D_{\bar{u}}^h) + e_d^2(D_d^h - D_{\bar{d}}^h)], \quad (22)$$

$$X_8^h = \frac{1}{6Y} [-e_u^2(D_u^h - D_{\bar{u}}^h) - e_d^2(D_d^h - D_{\bar{d}}^h) + 2e_s^2(D_s^h - D_{\bar{s}}^h)], \quad (23)$$

with

$$Y = \frac{1 + \gamma^2}{1 + R(x, Q^2)} \sum_a e_a^2 q_a(x; Q^2) D_a^h(Q^2). \quad (24)$$

The terms $A_{1,u}^h, A_{1,d}^h$ and $A_{1,s}^h$ contain the contributions of the sum of quark and antiquark distributions, which appear also in the inclusive polarized spin asymmetry (polarized structure functions), (14), and can therefore be measured independently in DIS. [Actually, in DIS with proton or nuclear targets one is able to measure directly only two flavor combinations of these three distributions; the third one can be inferred using $SU(3)$ symmetry arguments.] The term $A_{1,0}^h$ in (15) contains the flavor-singlet polarized antiquark distribution. The terms $A_{1,3}^h$ and $A_{1,8}^h$, finally, are proportional to the flavor-nonsinglet (triplet and octet, respectively) combinations of the polarized antiquark distributions, which do not contribute to inclusive DIS and are therefore left essentially unconstrained in the parametrizations of parton distributions derived from fits to inclusive data [2].

The decomposition (15) now allows us to consistently combine the information available from inclusive DIS, contained in the standard parametrizations of polarized parton distributions, with the results of our model calculation of the flavor asymmetries of the antiquark distributions, when computing the total semi-inclusive spin asymmetry. To evaluate the numerators of the contributions $A_{1,u}^h, A_{1,d}^h$ and $A_{1,s}^h$ we use the GRSV LO parametrizations of the distributions $\Delta u(x) + \Delta \bar{u}(x)$, $\Delta d(x) + \Delta \bar{d}(x)$, $\Delta s(x) + \Delta \bar{s}(x)$ [2].⁵ For the contribution $A_{1,0}^h$ involving the flavor-singlet antiquark distribution, $\Delta \bar{u}(x) + \Delta \bar{d}(x) + \Delta \bar{s}(x)$, we also use the GRSV LO parametrization, which is in good agreement with the result of the calculation in the chiral quark-soliton model [13]. To estimate the contributions of the flavor-asymmetric antiquark distributions to the spin asymmetry, $A_{1,3}^h$ and $A_{1,8}^h$, we take the results of the calculation in the chiral quark-soliton model, *cf.* Fig. 1 and (10), evolved from the scale of $\mu^2 = (600 \text{ MeV})^2$ up to the experimental scale. Note that in leading order $\Delta \bar{u}(x) - \Delta \bar{d}(x)$ and $\Delta \bar{u}(x) + \Delta \bar{d}(x) - 2\Delta \bar{s}(x)$ do not mix with the total distributions under evolution [we neglect $SU(3)$ -symmetry breaking effects due to the finite strange quark mass in the evolution]. Finally, to evaluate the denominators in (20)–(23), we use the GRV LO parametriza-

⁵ To be consistent with our treatment of $SU(3)$ flavor symmetry breaking in the model calculation we take the so-called “standard” scenario.

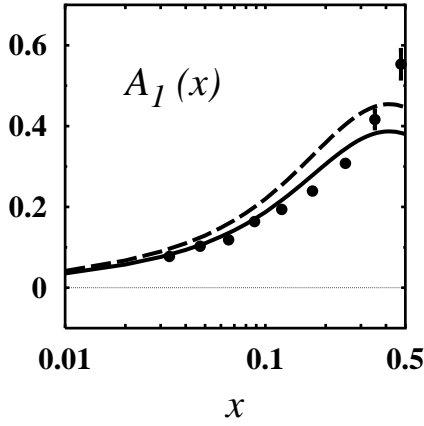


Fig. 6. The inclusive spin asymmetry, (14), evaluated with the GRSV/GRV parametrization for the polarized/unpolarized parton distributions, at $Q^2 = 2.5 \text{ GeV}^2$. *Solid line:* (14) evaluated without the explicit factor $[1 + R(x, Q^2)]$. *Dashed line:* same as solid line, but explicitly including the factor $[1 + R(x, Q^2)]$. *Dots:* HERMES data from [5]

tion of unpolarized parton distributions [31], which agrees well with the model calculations of [9, 10, 12, 13].

We emphasize that with the above “hybrid” set of polarized parton distributions we automatically fit *all inclusive data*, since the GRSV parametrization was determined from fits to the structure function data. In particular, the GRSV parametrization describes well the HERMES data for the inclusive spin asymmetry, (14), as can be seen from Fig. 6.⁶ Note that the HERMES data are in good agreement with the SLAC E143 data for the inclusive spin asymmetry [32].

Spin asymmetries in charged pion production. In order to determine the contributions of the various combinations of polarized quark and antiquark distributions to the semi-inclusive spin asymmetry, (12), we need to evaluate the coefficients X_u^h, \dots, X_s^h , (20)–(23), using a set of quark and antiquark fragmentation functions. Like the parton distributions, the fragmentation functions are process-independent quantities, which can in principle be determined from a variety of hard processes with hadronic final states, such as e^+e^- annihilation, or in semi-inclusive hadron production in unpolarized DIS. Unfortunately, experimental knowledge of fragmentation functions is still comparatively poor. This applies in particular to the so-called unfavored fragmentation functions, which we need to study the influence of flavor asymmetry in the antiquark distribution, see (22) and (23). The low-scale parametrizations of unpolarized quark and antiquark fragmentation functions of Binnewies *et al.*, which fit variety of e^+e^- annihilation and semi-inclusive DIS data, describe only fragmentation into positively and negatively charged particles combined, which is not sufficient for our purposes.

⁶ The GRSV parametrization was derived by fitting to the ratio (14) including the factor $[1 + R(x, Q^2)]$, so that this factor is contained in the polarized parton distribution functions and should not be included explicitly when evaluating (14). The effect of this factor is shown in Fig. 6.

Table 1. Rows 1 and 2: The coefficients (20)–(23) for π^+ and π^- production, evaluated with the HERMES fragmentation functions [8] for $z_{\min} = 0.2$. Rows 3 and 4: Same for charged hadron production. The kaon and proton fragmentation functions have been taken from the EMC measurements [7] (details see text). Rows 5 and 6: Same for kaon production only

	X_u^h	X_d^h	X_s^h	X_0^h	X_3^h	X_8^h
$h = \pi^+$	0.200	0.029	0.029	-0.021	-0.053	-0.011
π^-	0.115	0.050	0.029	0.021	0.053	0.011
$h = h^+$	0.277	0.040	0.035	-0.037	-0.077	-0.023
h^-	0.140	0.056	0.043	0.037	0.077	0.023
$h = K^+$	0.049	0.004	0.004	-0.008	-0.017	-0.008
K^-	0.016	0.004	0.012	0.008	0.017	0.008

The π^+ and π^- fragmentation functions separately have been extracted at low Q^2 from semi-inclusive pion production at HERMES [8]. The number of independent pion fragmentation functions is reduced by isospin and charge conjugation invariance:

$$D_u^{\pi^+} = D_{\bar{d}}^{\pi^+} = D_d^{\pi^-} = D_{\bar{u}}^{\pi^-} \equiv D, \quad (25)$$

$$D_d^{\pi^+} = D_{\bar{u}}^{\pi^+} = D_u^{\pi^-} = D_{\bar{d}}^{\pi^-} \equiv \tilde{D}, \quad (26)$$

where D and \tilde{D} are called, respectively, favored and unfavored fragmentation function. In addition, in [8] it was assumed that the strange quark fragmentation function into pions is approximately equal to the unfavored fragmentation function for u and d quarks:

$$D_s^{\pi^+} = D_{\bar{s}}^{\pi^-} \approx D_s^{\pi^+} = D_s^{\pi^-} \approx \tilde{D}. \quad (27)$$

With these assumptions we can compute the integrals (13) for $h = \pi^+, \pi^-$ using the HERMES fragmentation functions (extraction method 1, corrected for 4π acceptance) [8]. The values of the coefficients $X_u^{\pi^\pm}, \dots, X_8^{\pi^\pm}$ integrals obtained with a cutoff $z_{\min} = 0.2$ (the value used in the analysis of HERMES charged hadron data [5]) are given in rows 1 and 2 of Table 1. The numerical values of the coefficients reveal two things: First, the dominant contribution to the charged hadron asymmetry comes from the sum of the polarized u -quark and antiquark distributions in the target, $\Delta u(x) + \Delta \bar{u}(x)$, which is a consequence of the large squared charge of the u -quark. Second, among the various flavor combinations of the antiquark distributions the isovector one, $\Delta \bar{u}(x) - \Delta \bar{d}(x)$ enters with the largest coefficient — a fortunate circumstance for attempts to extract this distribution from the data.

The results for the spin asymmetry in semi-inclusive π^+ and π^- production are shown in Fig. 7. The dashed lines show the results obtained taking into account only the contributions $A_{1,u}^{\pi^\pm}, A_{1,d}^{\pi^\pm}, A_{1,s}^{\pi^\pm}$ and $A_{1,0}^{\pi^\pm}$ to the spin asymmetry, (15), i.e., what would be obtained without flavor asymmetry in the polarized antiquark distribution of the proton. The contributions $A_{1,3}^{\pi^\pm}$, proportional to $\Delta \bar{u}(x) - \Delta \bar{d}(x)$, are shown by the dotted lines. The total results for the asymmetries, including all contributions,

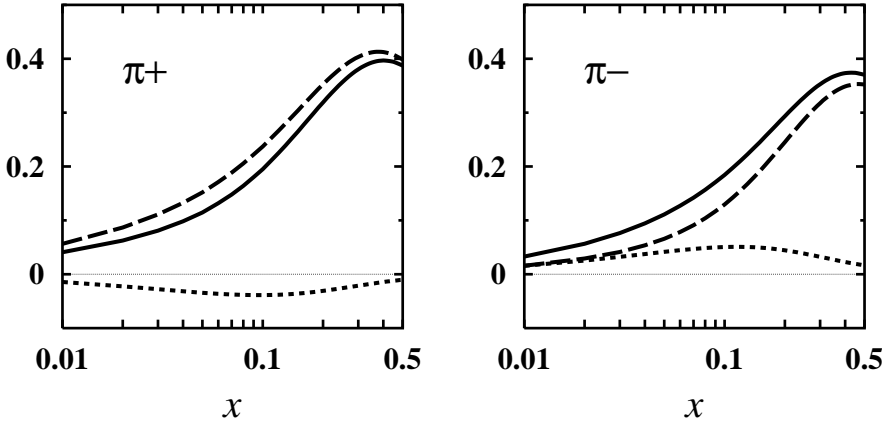


Fig. 7. The spin asymmetries for π^+ and π^- production in semi-inclusive DIS off the proton ($Q^2 = 2.5 \text{ GeV}^2$, $z_{\min} = 0.2$). *Dashed lines:* Sum of contributions $A_{1,u}^{\pi^+}$, $A_{1,d}^{\pi^+}$, $A_{1,s}^{\pi^+}$, and $A_{1,0}^{\pi^+}$ (and respectively for π^-), cf. (15). *Dotted lines:* Contributions $A_{1,3}^{\pi^+}$ and $A_{1,3}^{\pi^-}$, respectively, proportional to the flavor asymmetry $\Delta\bar{u}(x) - \Delta\bar{d}(x)$ in the target, evaluated with the distribution shown in Fig. 1. *Solid lines:* Total results, including the effect of $\Delta\bar{u}(x) - \Delta\bar{d}(x)$. The contributions $A_{1,8}^{\pi^+}$ and $A_{1,8}^{\pi^-}$ are very small and therefore not shown separately

are shown by the the solid lines. [The contributions $A_{1,8}^{\pi^\pm}$ are very small, of the order of 10% of $A_{1,3}^{\pi^\pm}$, and not shown separately.] One sees that in both cases the effect of the flavor asymmetry of the antiquark distribution is noticeable.

Spin asymmetries in charged hadron production and comparison with the HERMES data. We now turn to the spin asymmetries in charged production, which have been measured by the SMC [4] and HERMES [5] experiments. Unfortunately, no complete set of quark fragmentation functions for charged hadrons (K^+ , K^- , p , \bar{p}) at the HERMES scale ($Q^2 = 2.5 \text{ GeV}^2$) is available. We therefore take recourse to the older EMC results for the fragmentation functions [7], in which positively and negatively charged hadrons were separated. These data have been taken at a higher scale of $Q^2 = 25 \text{ GeV}^2$. Since it turns out that the dominant contribution to the semi-inclusive spin asymmetry for production of charged hadrons comes from the pions, we combine the HERMES result for the pion fragmentation functions [8] with the EMC fragmentation functions for kaons and protons [7], ignoring the scale dependence of the kaon and proton fragmentation functions, which anyway give a small contribution.⁷ Again, isospin and charge conjugation allow us to write:

$$D_u^{K^+} = D_{\bar{u}}^{K^-} \equiv D^K, \quad (28)$$

$$D_d^{K^+} = D_{\bar{d}}^{K^-} \equiv \tilde{D}^K, \quad (29)$$

$$D_u^p = D_{\bar{u}}^{\bar{p}} \equiv D^p, \quad (30)$$

$$D_{\bar{u}}^{\bar{p}} = D_u^p \equiv \tilde{D}^p. \quad (31)$$

Furthermore, following the analysis in [7], we shall assume that

$$D_s^{K^-} = D_{\bar{s}}^{K^+} \approx D^K, \quad (32)$$

$$D_s^{K^+} = D_{\bar{s}}^{K^-} \approx \tilde{D}^K, \quad (33)$$

⁷ In principle the evolution equations for fragmentation functions [33,34] would allow us to parametrize the EMC results in terms of fragmentation functions at a lower scale; however, in order to do so consistently we would need also the gluon fragmentation functions at the higher scale, which has not been measured by EMC.

$$D_d^p = D_{\bar{d}}^{\bar{p}} \approx D^p, \quad (34)$$

$$D_s^p = D_{\bar{s}}^{\bar{p}} \approx D_d^p = D_{\bar{d}}^{\bar{p}} = \tilde{D}^p. \quad (35)$$

With these assumptions all relevant fragmentation functions for $h^+ \approx \pi^+ + K^+ + p$ and $h^- \approx \pi^- + K^- + \bar{p}$ can be estimated in terms of the six functions D , \tilde{D} , D^K , \tilde{D}^K , D^p and \tilde{D}^p . Evaluating the integrals with $z_{\min} = 0.2$ (the cutoff used in the analysis of HERMES data [5]) we obtain the values shown in rows 3 and 4 of Table 1. One sees that the values are not too different from those obtained for π^+ and π^- production; only the sensitivity to the strange quark distributions has increased somewhat due to the inclusion of kaon production.

In Fig. 8 we show the results for the spin asymmetries in h^+ and h^- production. As in Fig. 7 for π^+ and π^- we plot the asymmetry that would be obtained without flavor asymmetry of the polarized antiquark distribution in the target ($A_{1,u}^{h^\pm} + A_{1,d}^{h^\pm} + A_{1,s}^{h^\pm} + A_{1,0}^{h^\pm}$), the contributions $A_{1,3}^{h^\pm}$ and $A_{1,8}^{h^\pm}$ containing the effect of the flavor asymmetry, and the total result.

A preliminary comparison of the theoretical results for $A_1^{h^\pm}$ shows that the spin asymmetries computed including the effects of $\Delta\bar{u}(x) - \Delta\bar{d}(x)$ (solid lines in Fig. 8) are consistent with the HERMES [5] and SMC [4] data. The accuracy of the present data, in particular for $A_1^{h^-}$, seems not to be sufficient for a definite choice between the theoretical results obtained with (solid lines) and without (dashed lines in Fig. 8) the flavor asymmetry of the polarized antiquark distribution. Also, one should be aware that there are several sources of uncertainty in our theoretical predictions. The greatest uncertainty comes from our imperfect knowledge of the fragmentation function, mostly from the pion fragmentation functions. In the analysis of [8], significant corrections were applied to the measured fragmentation functions in order to compensate for the acceptance of the HERMES detector. (We use the 4π -corrected fragmentation functions in our above estimates.) A full error analysis would require keeping track of the systematic error in the fragmentation functions and is outside the scope of this paper. One should consider the possibility of changing the above analysis such as to be able to work directly with the fragmentation functions specific to

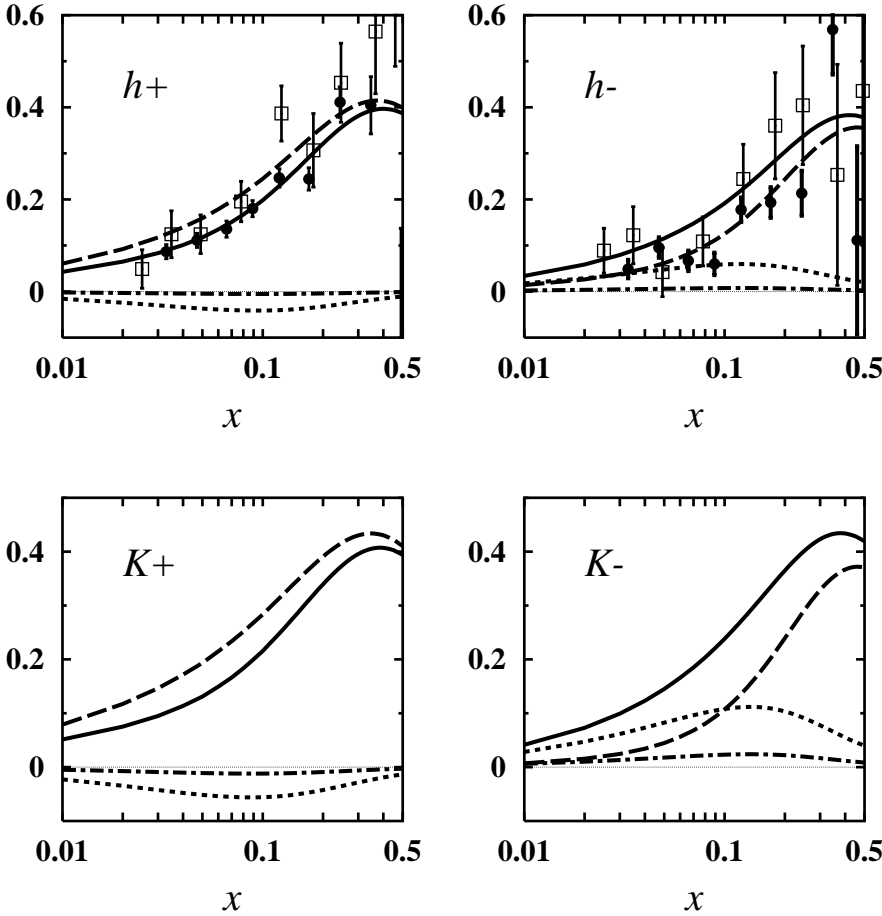


Fig. 8. The spin asymmetries for h^+ and h^- production in semi-inclusive DIS off the proton ($Q^2 = 2.5 \text{ GeV}^2$, $z_{\min} = 0.2$). *Dashed lines:* Sum of contributions $A_{1,u}^{h^+}$, $A_{1,d}^{h^+}$, $A_{1,s}^{h^+}$, and $A_{1,0}^{h^+}$ (and respectively for h^-), cf. (15). *Dotted lines:* Contributions $A_{1,3}^{h^+}$ and $A_{1,3}^{h^-}$, respectively, proportional to the flavor asymmetry $\Delta\bar{u}(x) - \Delta\bar{d}(x)$ in the target, evaluated with the distribution shown in Fig. 1. *Dash-dotted line:* Contributions $A_{1,8}^{h^+}$ and $A_{1,8}^{h^-}$, respectively. *Solid lines:* Total results, including the effect of flavor asymmetry of the polarized antiquark distribution. *Open Squares:* SMC data [4]. *Filled Circles:* HERMES data [5]

Fig. 9. The spin asymmetries for K^+ and K^- production in semi-inclusive DIS off the proton ($Q^2 = 2.5 \text{ GeV}^2$, $z_{\min} = 0.2$). *Dashed lines:* Sum of contributions $A_{1,u}^{K^+}$, $A_{1,d}^{K^+}$, $A_{1,s}^{K^+}$, and $A_{1,0}^{K^+}$ (and respectively for K^-), cf. (15). *Dotted lines:* Contributions $A_{1,3}^{K^+}$ and $A_{1,3}^{K^-}$, respectively, proportional to the flavor asymmetry $\Delta\bar{u}(x) - \Delta\bar{d}(x)$ in the target, evaluated with the distribution shown in Fig. 1. Note the large contribution in K^- production. *Dash-dotted line:* Contributions $A_{1,8}^{K^+}$ and $A_{1,8}^{K^-}$, respectively. *Solid lines:* Total results, including the effect of flavor asymmetry of the polarized antiquark distribution

the HERMES detector, avoiding the 4π corrections. It is conceivable that in this way one could significantly reduce the systematic error in the fragmentation functions.

Recently, Morii and Yamanishi have attempted to extract $\Delta\bar{u}(x) - \Delta\bar{d}(x)$ from the data for polarized semi-inclusive asymmetries by combining data taken with proton and Helium targets [35]. (It was shown in [19] that the asymmetry calculated in the chiral quark–soliton model is consistent with their bounds obtained in [35].) Since in the case of the HERMES experiment the statistics of the Helium data is significantly worse than for the proton, this combination of data results in a loss of accuracy. Also, this approach requires accurate compensation for nuclear binding effects. In contrast, our method of analysis relies on proton data only.

Spin asymmetries in charged kaon production. It is interesting to consider separately also the spin asymmetries in the production of charged kaons only. In particular, K^- cannot be produced by favored fragmentation of either u or d quarks in the target, which makes for the bulk contribution to the semi-inclusive spin asymmetry in π^\pm or h^\pm production. In this case one might expect a large sensitivity of the spin asymmetry to the flavor asymmetries of the polarized antiquark distributions. For a rough estimate we can use the EMC fragmentation functions to evaluate the coefficients (20)–(23) for K^+ and K^- ; the

results are shown in rows 5 and 6 of Table 1. The contributions to the spin asymmetries are shown in Fig. 9. One sees that, in particular in the case of K^- production, the contribution proportional to $\Delta\bar{u}(x) - \Delta\bar{d}(x)$ in the proton is large. Thus, semi-inclusive charged kaon production could be a sensitive test of the flavor decomposition of the antiquark distribution in the nucleon.

5 Conclusions and outlook

Starting from the observation that the $1/N_c$ -expansion predicts large flavor asymmetries of the polarized antiquark distributions, and the quantitative estimates for $\Delta\bar{u}(x) - \Delta\bar{d}(x)$ and $\Delta\bar{u}(x) + \Delta\bar{d}(x) - 2\Delta\bar{s}(x)$ obtained from the chiral quark–soliton model, we have explored several consequences of a large flavor asymmetry of the polarized antiquark distributions.

On the theoretical side, we have argued that the very small value for the polarized antiquark flavor asymmetry obtained from polarized rho meson exchange in the meson cloud picture [20] does not rule out a large asymmetry, since polarized rho meson exchange is by far not the dominant contribution to $\Delta\bar{u}(x) - \Delta\bar{d}(x)$ in that approach. Comparison with the large- N_c result suggests that, in the terms of the meson cloud model, a large contribution is likely to come from the interference of pion and “sigma

meson” exchange. It could be interesting to explore this qualitative suggestion in more detail within the meson cloud picture.

As to experimental consequences, we have found that the large flavor asymmetry predicted by the chiral quark soliton model is consistent with the recent HERMES data on spin asymmetries in semi-inclusive charged hadron production. Our conclusions are based on the presently available information on quark and antiquark fragmentation functions; however, to the extent that we have explored it, they seem to be robust with regard to the systematic uncertainties in the fragmentation functions. We do not claim that at the present level of accuracy the HERMES data for $A_1^{h\pm}$ necessitate a large flavor asymmetry of the antiquark distribution in the proton. However, assuming a large flavor asymmetry we obtain a good fit to the data. In this sense the HERMES results should not be seen as evidence for a small flavor asymmetry of the polarized antiquark distribution. Also, we have argued that the assumption $\Delta\bar{u}(x)/\bar{u}(x) = \Delta\bar{d}(x)/\bar{d}(x)$ made in the analysis of the HERMES data in [5] artificially limits the contributions from the polarized antiquark flavor asymmetry, and thus does not constitute a real alternative to the reference fit assuming zero flavor asymmetry.

At present, one source of uncertainty in our theoretical results are the systematic errors in the HERMES quark and antiquark fragmentation functions introduced by the corrections for 4π acceptance. It would be worthwhile to investigate if not the above analysis could be carried out directly with the fragmentation functions for HERMES acceptance, which could considerably reduce the systematic error.

We have shown that the flavor asymmetry of the polarized antiquark distribution makes a particularly large contribution to the spin asymmetries in charged kaon production. Such measurements could be an interesting option with detectors which allow discrimination between pions and kaons in the final state, e.g. at HERMES or CEBAF.

Acknowledgements. The authors are grateful to A. Schäfer and M. Strikman, from discussions with whom arose the idea to write this note, and to M. Düren for comments. Helpful hints from Ph. Geiger, R. Jakob, B. Kniehl, L. Mankiewicz, P.V. Pobylitsa, and P. Schweitzer are also gratefully acknowledged. This work has been supported in part by the Deutsche Forschungsgemeinschaft (DFG), by a joint grant of the DFG and the Russian Foundation for Basic Research, by the German Ministry of Education and Research (BMBF), and by COSY, Jülich.

References

1. COMPASS Collaboration (G. Baum et al.), “COMPASS: A proposal for a common muon and proton apparatus for structure and spectroscopy”, CERN-SPSLC-96-14 (1996)
2. M. Glück, E. Reya, M. Stratmann, W. Vogelsang, Phys. Rev. D **53**, 4775 (1996)
3. L.L. Frankfurt, M.I. Strikman, L. Mankiewicz, A. Schäfer, E. Rondio, A. Sandacz, and V. Papavassiliou, Phys. Lett. B **230**, 141 (1989)
4. Spin Muon Collaboration (B. Adeva et al.), Phys. Lett. B **420**, 180 (1998); Phys. Lett. B **369**, 93 (1996)
5. HERMES Collaboration (K. Ackerstaff et al.), “Flavor decomposition of the polarized quark distributions in the nucleon from inclusive and semi-inclusive deep inelastic scattering”, Report DESY-99-048, hep-ex/9906035
6. J. Binnewies, B.A. Kniehl, G. Kramer, Z. Phys. C **65**, 471 (1995)
7. European Muon Collaboration (M. Arneodo et al.), Nucl. Phys. B **321**, 541 (1989)
8. Ph. Geiger, “Measurement of Fragmentation Functions at HERMES”, Doctoral Dissertation, Heidelberg University (1998)
9. D.I. Diakonov, V.Yu. Petrov, P.V. Pobylitsa, M.V. Polyakov, C. Weiss, Nucl. Phys. B **480**, 341 (1996)
10. D.I. Diakonov, V.Yu. Petrov, P.V. Pobylitsa, M.V. Polyakov, C. Weiss, Phys. Rev. D **56**, 4069 (1997)
11. For a more detailed discussion of the flavor asymmetries, see: B. Dressler, K. Goetze, P.V. Pobylitsa, M.V. Polyakov, T. Watabe, C. Weiss, in: Proceedings of the 11th International Conference on Problems of Quantum Field Theory, Dubna, Russia, Jul. 13–17, 1998, hep-ph/9809487
12. P.V. Pobylitsa, M.V. Polyakov, K. Goetze, T. Watabe, C. Weiss, Phys. Rev. D **59**, 034024 (1999)
13. M. Wakamatsu, T. Kubota, Phys. Rev. D **60**, 034020 (1999)
14. New Muon Collaboration (P. Amaudruz et al.), Phys. Rev. Lett. **66**, 2712 (1991); New Muon Collaboration (M. Arneodo et al.), Phys. Rev. D **50**, R1 (1994); Phys. Lett. B **364**, 107 (1995)
15. K. Gottfried, Phys. Rev. Lett. **18**, 1174 (1967)
16. For a recent review, see: S. Kumano, Phys. Rept. **303**, 183 (1998)
17. FNAL E866/NuSea Collaboration (E.A. Hawker et al.), Phys. Rev. Lett. **80**, 3715 (1998); FNAL E866/NuSea Collaboration (J.C. Peng et al.), Phys. Rev. D **58**, 092004 (1998)
18. HERMES Collaboration (K. Ackerstaff et al.), Phys. Rev. Lett. **81**, 5519 (1998)
19. M. Wakamatsu, T. Watabe, Report OU-HEP-324, hep-ph/9908425
20. R.J. Fries, A. Schäfer, Phys. Lett. B **443**, 40 (1998)
21. K.G. Boreskov, A.B. Kaidalov, Eur. Phys. J. C **10**, 143 (1999)
22. J.D. Sullivan, Phys. Rev. D **5**, 1732 (1972)
23. A.W. Thomas, Phys. Lett. **126 B**, 97 (1983); L.L. Frankfurt, L. Mankiewicz, M.I. Strikman, Z. Phys. A **334**, 343 (1989); E.M. Henley, G.A. Miller, Phys. Lett. B **251**, 453 (1990); W.Y.P. Hwang, J. Speth, G.E. Brown, Z. Phys. A **339**, 383 (1991); W. Melnitchouk, A.W. Thomas, Phys. Rev. D **47**, 3794 (1993); H. Holtmann, N.N. Nikolaev, J. Speth, A. Szczurek Z. Phys. A **353**, 411 (1996); H. Holtmann, A. Szczurek, J. Speth, Nucl. Phys. A **596**, 397 (1996), *ibid.* 631
24. E. Witten, Nucl. Phys. B **223**, 433 (1983)
25. D. Diakonov, V. Petrov, Nucl. Phys. B **272**, 457 (1986); D. Diakonov, V. Petrov, LNPI preprint LNPI-1153 (1986), published (in Russian) in: Hadron Matter under Extreme Conditions, Naukova Dumka, Kiev (1986), p. 192

26. D.I. Diakonov, V.Yu. Petrov, P.V. Pobylitsa, Nucl. Phys. B **306** (1988) 809; For a review of the foundations of this model see: D.I. Diakonov, Lectures given at the Advanced Summer School on Nonperturbative Quantum Field Physics, Peniscola, Spain, Jun. 2–6 1997. Published in: Peniscola 1997: Advanced school on non-perturbative quantum field physics, p. 1, hep-ph/9802298
27. M.V. Polyakov, Yad. Fiz. **51**, 1110 (1990) [Sov. J. Nucl. Phys. **51**, 711 (1990)]; A. Blotz et al., Nucl. Phys. A **555**, 765 (1993)
28. D. Diakonov, V. Petrov, M. Polyakov, Z. Phys. A **359**, 305 (1997)
29. W. Koepf, L.L. Frankfurt, M. Strikman, Phys. Rev. D **53**, 2586 (1996)
30. M. Penttinen, M.V. Polyakov, K. Goeke, Report RUB-TPII-19/98, hep-ph/9909489
31. M. Glück, E. Reya, A. Vogt, Z. Phys. C **67**, 433 (1995)
32. E143 Collaboration: K. Abe et al., Phys. Rev. D **58**, 112003 (1998)
33. V.N. Gribov, L.N. Lipatov, Sov. J. Nucl. Phys., **15**, 438 (1972); Y.L. Dokshitzer, Sov. Phys. JETP, **46**, 641 (1977)
34. M. Stratmann, W. Vogelsang, Nucl. Phys. B **496**, 41 (1997)
35. T. Morii, Y. Yamanishi, Report KOBE-FHD-00-01, FUT-99-01, hep-ph/9905294